

Chapter 4

Analysis of cells lacking various p85 isoforms

ABSTRACT

Many lines of evidence suggest that the phosphoinositide 3-kinase (PI3K) pathway is required for actin rearrangement induced by PDGF. However, as discussed in the previous chapter the evidence comes from experiments with drug inhibitors that affect all forms of PI3K as well as other lipid and protein kinases, or from receptor mutations or overexpression of dominant-negative forms of PI3K, each of which can affect multiple signaling pathways downstream of the PDGF receptor. Here, we describe the use of p85^{-/-}-p55^{-/-}-p50^{-/-}-p85^{-/-} mouse embryonic fibroblasts (MEFs) to analyze the requirement for the class Ia PI3K regulatory isoform p85 in PDGF-induced lamellipodia formation and cell migration. We show that fibroblasts deficient in all p85^{-/-} and p85^{-/-} gene products (p85^{-/-}-p55^{-/-}-p50^{-/-}-p85^{-/-}) are defective in lamellipodia formation and cell migration upon PDGF stimulation. Rac has been shown to mediate PDGF induced lamellipodia formation (Hawkins et al., 1995). We find that in MEFs lacking p85^{-/-} and p85^{-/-} PDGF fails to activate Rac. Transient overexpression of the Rac specific GDP-GTP exchange factor (GEF) Vav2 in p85^{-/-}-p55^{-/-}-p50^{-/-}-p85^{-/-} fibroblasts is sufficient to rescue the defect and to cause membrane ruffling following PDGF treatment. Reintroduction of p85^{-/-}, or p85^{-/-} to the p85^{-/-}-p55^{-/-}-p50^{-/-}-p85^{-/-} MEFs restored PDGF-dependent lamellipodia formation. More significantly, reintroduction of p50^{-/-} (which lacks the Rho-GAP homology domain that interacts with rho/rac/cdc42 family members) also restored PDGF-dependent lamellipodia formation. These results show that class Ia PI3K is critical for PDGF-dependent actin rearrangement but that the rho/rac/cdc42-interacting domain of p85 is not required for this response.

INTRODUCTION

Role of PI3K in actin rearrangement & cell motility

The rearrangement of filamentous actin structures is fundamental to dynamic processes such as cell motility. Cell migration plays important roles in development, in immune response (e.g. to allow leukocytes to travel to sites of infection), and in woundhealing. In addition, aberrant motility in cancer cells promotes their metastasis. Cell movement is a complex process that requires the cell to interpret chemotactic cues in the external environment in order to polarize its front to generate a leading edge. In a resting cell, the actin cytoskeleton anchors the cell to the substratum via large contractile bundles of actin myosin filaments known as stress fibers and focal adhesions. In order to move, the cell first generates actin-based finger-like protrusions called filopodia that extend from the cell. Subsequently, these protrusions become networked and generate an edge. This structure, called lamella, consists of highly motile ruffles. The leading edge of the cell pushes forward and establishes new contacts with the substratum, while the rear of the cell loses its contacts and retracts. PI3K activity has been shown to be a crucial regulator of cell migration at the level of cell polarization and lamellipodia formation. However, it is not well understood what roles the various PI3K regulatory isoforms play in these processes.

By using PI3K-inhibitors wortmannin or LY294002, or by overexpressing dominant-negative forms of p85, or by the expression of PDGF receptor mutants deficient in binding and activating PI3K, it has been argued that PDGF-induced cell ruffling and chemotaxis occurs in a PI3K dependent manner (Severinsson et al., 1990b), (Wennstrom et al., 1994a), (Wennstrom et al., 1994b), (Kundra et al., 1994). These data suggest that recruitment and activation of PI3K is required for PDGF mediated ruffling and migration. Hawkins identified the small GTPase Rac as the crucial mediator of PI3K signaling (Hawkins et al., 1995). In this chapter, we show that cells deleted for class Ia PI3K isoforms are impaired in PDGF-induced cell ruffling and migration and that this defect is attributed to decreased PDGF-induced Rac activation. Rac proteins belong to the Rho family of GTPases. The effects of the Rho family of GTPases on actin

rearrangement have been characterized in fibroblasts by microinjection of living cells. Microinjection of Rho leads to stress fiber formation and the enhancement of focal adhesions (Ridley and Hall, 1992). Injection of the small GTPase Rac results in ruffling, whereas injection of dominant negative Rac blocks PDGF-induced ruffling (Ridley and Hall, 1992). Microinjection of Cdc42 into Swiss 3T3 fibroblasts leads to rapid formation of filopodia (Severinsson et al., 1990a). The polymerized actin in lamellipodia or filopodia are associated with focal contacts that differ from Rho-induced focal adhesion complexes (reviewed in (Nobes and Hall, 1994). Rac proteins are inactive when GDP is bound and active in their GTP-bound form. In resting cells, GDP dissociation inhibitors (GDIs) sequester Rac-GDP in the cytosol. Following release from the GDI, Rac-GDP inserts itself into the plasma membrane via its C-terminal prenyl moiety. The membrane bound guanyl exchange factor (GEF) now has access to Rac and promotes dissociation of GDP by opening the nucleotide-binding site. Since the concentration of GTP is much higher in the cytosol than GDP, Rac preferably binds GTP. Only the GTP-bound, active form of Rac interacts with its target proteins. All GEFs of the Rho family contain DH (Dbl homology) domains and PH domains. Some of these PH domains bind phosphoinositides, and might therefore mediate PI3K-dependent GTP loading of Rac by directly interacting with PI3K lipid products. Moreover, constitutively active mutants of p110 α promote the rearrangement of actin filaments in a manner similar to that observed in response to activated Rac (Reif et al., 1996). The hypothesis of PI3K being upstream of Rac rather than downstream is further supported by the fact that constitutively active Rac causes ruffling, even when PI3K is inhibited by wortmannin (Nobes et al., 1995). Most likely, PI3K activates Rac by activating its upstream GEFs. In this chapter we show that cells lacking class Ia PI3K are impaired in PDGF-induced ruffling due to defective Rac activation and that this defect can be restored by overexpression of the rac-specific GEF Vav2 (described below).

A variety of GEFs have been shown to act specifically on Rac. The Vav family (Vav 1-3) is the best studied of all Rac-GEFs. Tyrosine phosphorylation of Vav1 by various Src and Syk protein-tyrosine kinases is sufficient to activate its Rac-GEF activity (Crespo et al., 1997). It is hypothesized that the binding of PIP₃ to the PH domain of Vav1 relieves an intramolecular inhibition between its PH and DH domains, allowing the

phosphorylation of Tyr174 that further opens the DH/PH domains (Han et al., 1998), (Das et al., 2000). However, this mechanism has not been critically tested. It has been reported that activation of the more widely expressed Vav2 by EGF requires PI3K activity (Tamas et al., 2003). However, it is clear that Vav2 is not universally responsible for PI3K-dependent Rac activation since Vav2-deficient embryonic stem cells are still capable of PI3K-induced membrane ruffling (Welch, unpublished data).

Sos, a protein with both a Rac-GEF domain and a Ras-GEF domain is another candidate for mediating PI3K-dependent Rac activation. The N-terminal PH domain of Sos binds PIP₃ 3-fold better than PI-4,5-P₂ and thus might mediate a PIP₃-dependent effect on Sos location or activation. *In vivo*, the pool of Sos1 associated with E3b1/Abi1 and Eps8 (Epidermal growth factor receptor kinase substrate 8) exhibits specific Rac-GEF activity downstream of receptor-tyrosine kinases (Scita et al., 1999), (Scita et al., 2001). In a collaboration, using the p85 mutant cells that we have established, Innocenti et al. has shown, that the Rac-GEF activity of Sos seems to depend on the recruitment of class Ia PI3K to the Sos/Abi1/Eps8 trimeric complex through a still unclear mechanism that involves E3b1/Abi1. Furthermore, the necessity for PI3K recruitment can be bypassed by the direct addition of the PI3K lipid product PIP₃ (Innocenti et al., 2003).

Other GEFs that might mediate PI3K-dependent activation of Rac include SWAP-70 (Shinohara et al., 2002), Tiam1, (Fleming et al., 2000), aPIX (Yoshii et al., 1999) and the recently discovered P-Rex 1, which is mainly expressed in neutrophils. It has been shown that the binding of PIP₃ and the $\beta\gamma$ subunits of heterotrimeric G-proteins are required for the activation of P-Rex1. P-Rex1 hence serves as a coincidence detector for the activation of G-protein coupled receptors and PI3K in directing actin cytoskeleton rearrangement in neutrophils (Welch et al., 2002).

In addition to the evidence that PI3K activates Rac indirectly via its GEFs other studies have suggested that PIP₃ can bind Rac directly with a EC₅₀ around 50 μ M and promote its GDP dissociation in a dose dependent manner without affecting the loading of GTP (Missy et al., 1998).

Using green fluorescent protein-tagged Akt pleckstrin homology domain (GFP-AktPH) as a sensor for PIP₃, several laboratories have shown that PIP₃ is concentrated at the leading edge of migrating cells (Haugh et al., 2000), (Rickert et al., 2000), (Stephens

et al., 2002). Using a FRET-based biosensor approach, Gardiner et al showed the existence of a gradient of Rac in neutrophils: Rac is dynamically activated in the leading edge as well as in the retracting tail of a moving cell (Gardiner et al., 2002). Thus, Rac activation might be PI3K-dependent in the leading edge and adhesion-dependent in the rear of the cell. Recently, the existence of a positive feedback loop in neutrophils has been demonstrated, whereby Rac, activated by PI3K, causes further activation of PI3K (Weiner et al., 2002), (Srinivasan et al., 2003). Weiner et al. hypothesize that this positive feedback loop produces an asymmetry of PIP₃ (high concentration at cell front) that commits the cell to form only one leading edge to ensure fast responsiveness.

There is also evidence that PI3K can function downstream of Rac (Keely et al., 1997), (Inabe et al., 2002), (Sachdev et al., 2002). In addition, the GTP-bound form of Rac can interact with the Rho-GAP domain of p85 (Bokoch et al., 1996), (Tolias et al., 1995), (Zheng et al., 1994). Since the p85 Rho-GAP domain lacks GAP activity, such interaction might actually protect Rac from other GAPs. Conversely such interaction may augment PI3K activity (Zheng et al., 1994), (Bokoch et al., 1996), (Tolias et al., 1995). These results suggested the possibility that the positive feedback loop between Rac and PI3K might be mediated via the interaction between Rac and the Rho-GAP domain of p85. Since only p85 α and p85 β , but not p50 α , p55 α or p55 β contain this domain, deletion of the p85 α and p85 β isoforms would be expected to disrupt this feedback loop and re-addition of the full length p85 isoforms but not the shorter isoforms (e.g. p50 α) would be expected to restore this function. Furthermore, since the Rho-GAP domain is the least conserved domain between p85 α and p85 β (42% homology), this raises the possibility that there might exist a difference in Rac-GTP binding between p85 α and p85 β and hence, their abilities to direct actin rearrangement.

In this chapter, we will show that mouse embryonic fibroblasts lacking p85 α /p55 α /p50 α /p85 β (p85 mutant cells) are impaired in PDGF-induced ruffling and migration. Analysis of p85 α ^{-/-}p85 β ^{+/+} or p85 α ^{+/+}p85 β ^{-/-} cells or retroviral reintroduction of p85 α or p85 β into p85 α ^{-/-}p55 α ^{-/-}p50 α ^{-/-}p85 β ^{-/-} cells is sufficient to recover these cellular functions comparable to wild-type. Surprisingly, reintroduction of p50 α , which lacks the N-terminal SH3 domain, Rho-GAP domain and proline rich regions of p85 α or p85 β is sufficient to restore PDGF and IGF-1 induced membrane

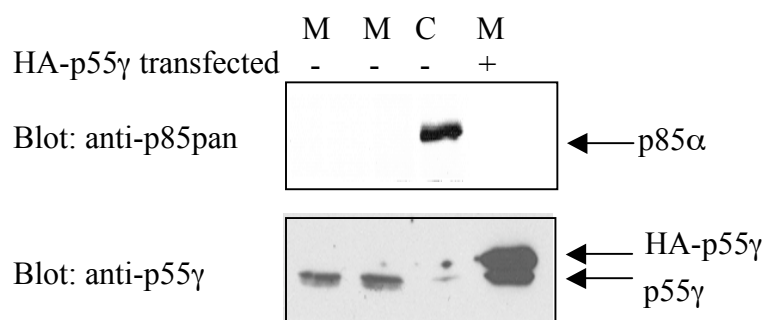
ruffling. We conclude that class Ia PI3K is required for PDGF-induced cell polarization, lamellipodia formation and cell migration. Furthermore, the C-terminal domains of p85 isoforms (SH2 domains and p110-binding site) but not the N-terminal domains of p85 α and p85 β are required for cellular ruffling.

RESULTS

Mouse embryonic fibroblasts (MEFs) lacking p85 α , p55 α , p50 α and p85 β fail to proliferate unless immortalized with SV40. Mice deficient in all gene products of p85 α and p85 β (p85 α ^{-/-}p55 α ^{-/-}p50 α ^{-/-}p85 β ^{-/-}) die during early embryonic development (described in the previous chapter). Therefore, the role of PI3K isoforms was studied in *ex vivo* experiments. MEFs from p85 α ^{-/-}p55 α ^{-/-}p50 α ^{-/-}p85 β ^{-/-} embryos (E8.5) and littermate control p85 α ^{+/-}p55 α ^{+/-}p50 α ^{+/-}p85 β ^{-/-} embryos were generated¹. While the control primary cells could be expanded, the p85 α ^{-/-}p55 α ^{-/-}p50 α ^{-/-}p85 β ^{-/-} primary cells stopped proliferating after about five passages and became senescent. This observation points to an important role of PI3K activity in preventing senescence. In order to establish cell lines the primary pools were immortalized by retroviral expression of the SV40 large T antigen. Doing so, 3 independent cell pools derived from p85 α ^{-/-}p55 α ^{-/-}p50 α ^{-/-}p85 β ^{-/-} embryos (from now on named mutant or “M”) and one control cell pool derived from a p85 α ^{+/-}p55 α ^{+/-}p50 α ^{+/-}p85 β ^{-/-} (from now on named control or “C”) littermate embryo were established. The expression levels of p85 isoforms were analyzed by western blot analysis and *in vitro* PI3K assays. Exponentially growing cells were lysed and the proteins were separated by SDS-PAGE and then probed with anti-p85pan or anti-p55 α antibodies. As a positive control for the anti-p55 α antibody, mutant cells were transfected with HA-p55 α (Fig. 8a, lower panel, lane 4). Western blot analysis of normalized total cell lysates showed complete loss of p85 α or p85 β in the mutant cells as expected (Figure 8a, upper panel). The smaller isoforms, p55 α and p50 α , are not detected in fibroblasts in general. Surprisingly, p55 α which is mainly expressed in brain (Pons et al., 1995), was substantially upregulated in the mutant cell pools. As expected p55 α was not detected in the control cells (Figure 8a, lower panel).

¹The probability of obtaining p85 α ^{-/-}p55 α ^{-/-}p50 α ^{-/-}p85 β ^{-/-} embryos from p85 α ^{+/-}p55 α ^{+/-}p50 α ^{+/-}p85 β ^{+/-} intercrosses is 1/16. Although there is a possibility of obtaining both wild-type and the desired mutant littermates from the same pregnancy, the odds are low. Therefore, cell lines from p85 α ^{+/-}p55 α ^{+/-}p50 α ^{+/-}p85 β ^{-/-} intercrosses were also derived.

A. p85 Protein Levels



B. p85-associated PI3K Activity

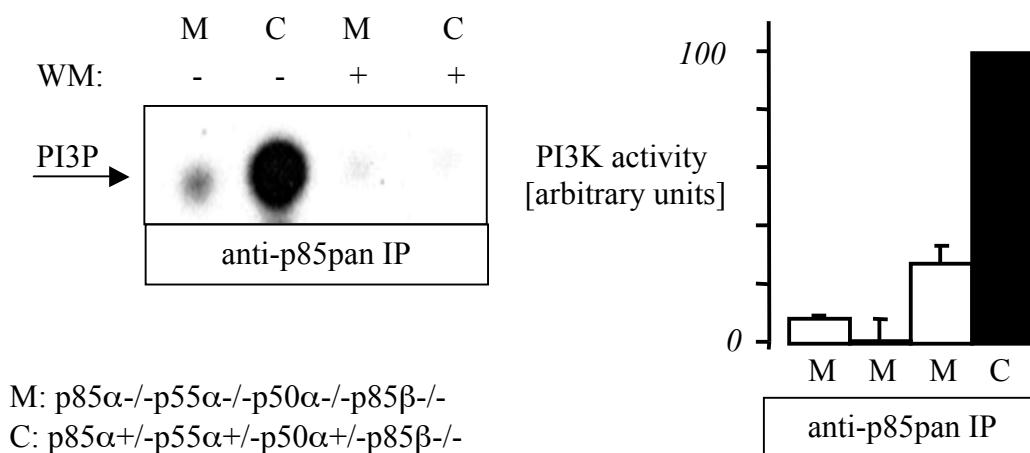


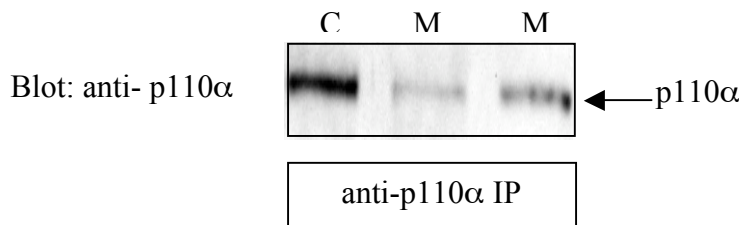
Fig. 8. Loss of all p85 \square and p85 \square gene products is associated with increased expression of p55 \square

A. HA-p55 \square was transfected into a mutant cell pool (M). The next day growing MEFs of the indicated genotypes were lysed and equal amounts of protein were subjected to SDS-PAGE and immunoblotted with anti-p85pan (upper panel) or anti-p55 \square antisera (lower panel). Figure 8a shows one out of three independent experiments. B. Growing MEFs of the indicated genotypes were lysed and equal amounts of protein were immunoprecipitated with anti-p85pan antibody. The immunoprecipitates were subjected to in vitro PI3-kinase assay with phosphoinositol as a substrate. Panel 8b (left) shows a representative radiograph with one mutant cell pool (M) and one control cell pool (C). A duplicate set was pretreated with 100nM wortmannin for 20min to inhibit the reaction. Panel 8b (right) shows a quantification of three independent experiments described in panel 8b (left), using 3 different mutant cell pools (M) and 1 control cell pool (C).

A further assessment of class Ia PI3K in the cells was made by measuring PI3K activity in anti-p85 immunoprecipitates from control cells and three different cell lines deleted for all forms of p85 α and p85 β . The amount of PI3K activity varied between the three mutant pools and was about 5-20% of the control cell pool (Figure 8b). The anti-p85pan antibody was raised against the N-terminal SH2 domain in the C-terminus of p85 α . This domain is highly homologous among all PI3K regulatory isoforms and hence this antibody recognizes all p85 isoforms including p55 α . The residual PI3K activity in the mutant cell lines is apparently explained by the upregulation of p55 α in these cells.

As described previously, p110 α stability is enhanced by its association with the regulatory subunit (Yu et al., 1998). Therefore, p110 α protein levels and kinase activity were assessed on immunoprecipitates of mutant and control cell pools using anti-p110 α antibodies. The immunoprecipitates were then either subjected to SDS-PAGE and western blot analysis using an anti-p110 α antibody or the immunoprecipitates were subjected to *in vitro* PI3K assays. Consistent with greatly reduced p85 levels, the protein level of p110 α was significantly decreased as well (Figure 9a). The p110 α activity was diminished to about 30-40% in the three different mutant cell pools compared to control cells as judged by *in vitro* PI3K assays (Figure 9b).

A. p110 α Protein Levels



B. p110 α Kinase Activity

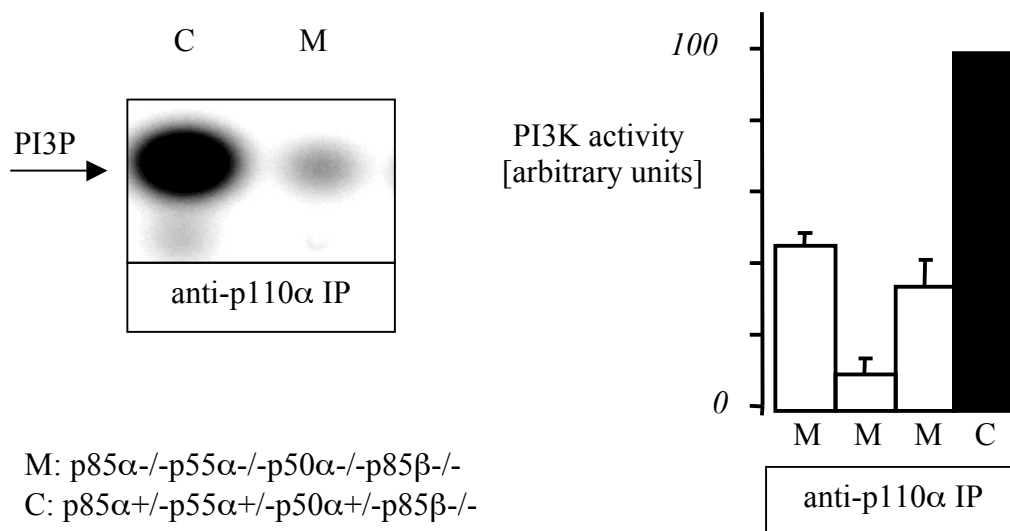
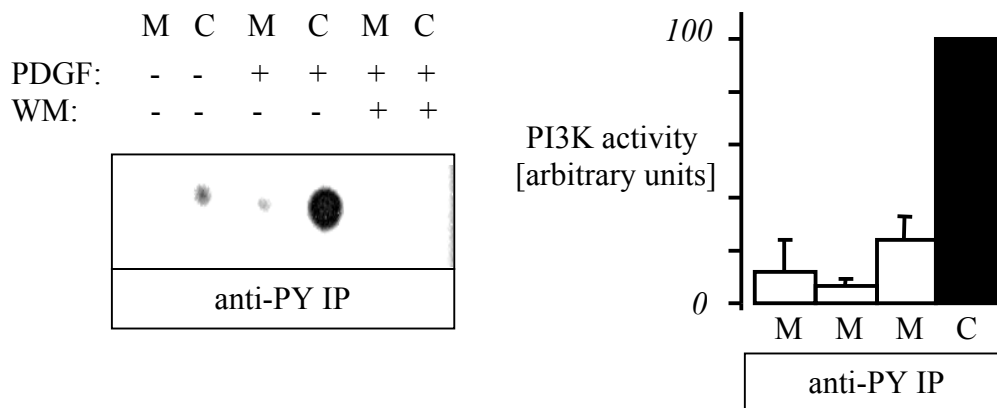


Fig. 9. Reduced expression of p110 α in MEFs lacking all p85 α and p85 β gene products.

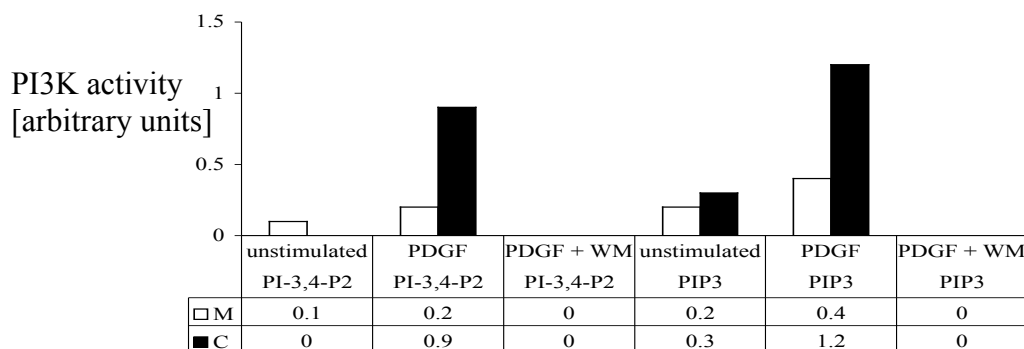
A. Growing MEFs of the indicated genotypes were lysed and equal amounts of protein were immunoprecipitated with an antibody specific for p110 α . The immunoprecipitates were subjected to SDS-PAGE and probed with anti-p110 α antibody. Equal loading was verified by detecting similar amounts of Erk on the same membrane (data not shown). Panel 9a shows a representative immunoblot with one control pool (C) and two mutant pools (M). B. Growing MEFs of the indicated genotypes were lysed and equal amounts of protein were immunoprecipitated with anti-p110 α antibody. The immunoprecipitates were subjected to in vitro PI3-kinase assay with PI as a substrate. Panel 9b (left) shows a representative radiograph on one control pool (C) and one mutant pool (M). Panel 9b (right) shows a quantification of three independent experiments described in panel 9b (left) using 3 mutant pools (M) and 1 control pool (C).

Activation of the PDGF receptor results in the recruitment of p85/p110 from the cytosol to the plasma membrane via the binding of p85 SH2 domains to phosphotyrosine residues on the PDGF receptor (Cantley et al., 1991), (Hawkins et al., 1992). This brings PI3K to close proximity with its lipid substrates. The fraction of PI3K that is actually recruited to the plasma membrane and therefore responsible for PIP₃ production following PDGF-BB stimulation can be assessed by *in vitro* kinase assay on anti-phosphotyrosine immunoprecipitates (which brings down activated PDGF receptor-PI3K complexes). In order to elucidate the contribution of the residual class Ia PI3K (p55 and associated p110 isoforms) in PDGF stimulated PI3K activity, the amount of PI3K activity recruited to phosphotyrosine residues after PDGF-BB treatment was assessed. Therefore, subconfluent serum-starved MEFs were stimulated for 5min with 10ng/ml PDGF-BB with or without wortmannin (100nM) pretreatment. The cells were lysed, immunoprecipitated with anti-phosphotyrosine antibody and then subjected to *in vitro* PI3K assays. Only about 10%-15% of the PI3K activity recruited in control cells was detected in the mutant cells and this activity could be completely blocked with wortmannin pretreatment (Figure 10a). We also analyzed the generation of class Ia PI3K lipid products after PDGF-BB treatment, *in vivo*. Therefore, subconfluent serum-starved mutant and control cell pools were labeled with radioactive orthophosphate and then stimulated for 5min with 10ng/ml PDGF-BB with or without wortmannin (100nM) pretreatment. The cells were lysed and then the lipids were extracted and analyzed by HPLC. Consistent with the *in vitro* data, PDGF-BB stimulation caused a reduced but still detectable production of both class Ia PI3K lipid products. About 20% PI-3,4-P₂ and about 30% PIP₃ were generated in comparison to control cells. Both activities were completely abolished when the cells were pretreated for 30min with 100nM wortmannin (Fig. 10b).

A. In vitro Generation of PI3K Products



B. In vivo Generation of PI3K Products



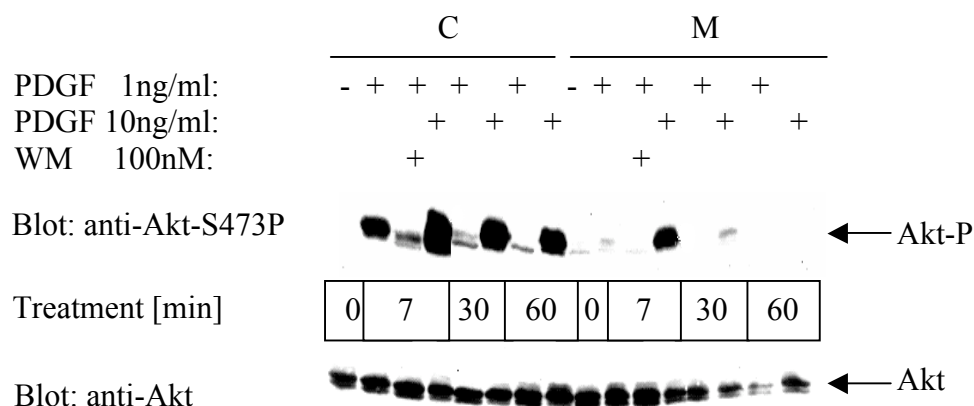
M: p85^{-/-}p55^{-/-}p50^{-/-}p85^{-/-}

C: p85^{+/+}p55^{+/+}p50^{+/+}p85^{-/-}

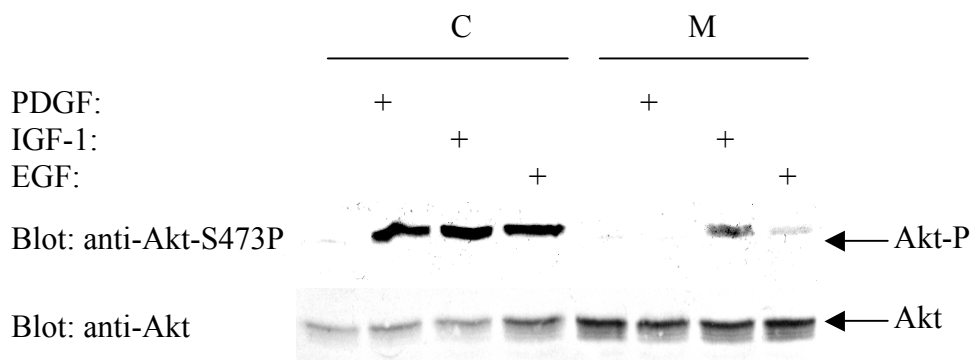
Fig. 10. Loss of all p85⁺ and p85⁻ gene products results in greatly reduced PDGF-stimulated PI3K activity *in vitro* and *in vivo*. A, Growing MEFs of the indicated genotypes were starved and then stimulated for 5min with 10ng/ml PDGF (+/- pretreatment with 100nM WM for 20min). Equal amounts of protein were immunoprecipitated with anti-PY (4G10) and then an *in vitro* PI3-kinase assay was performed. Left panel shows a representative experiment with one control clone and one mutant clone. Right panel shows the fold increase of PDGF stimulated PI3K activity of three mutant pools in comparison to one control pool (result of three independent experiments). B, Growing MEFs of the indicated genotypes were starved, metabolically labeled with ³²PO₄ and then stimulated for 5min with 10ng/ml PDGF (+/- pretreatment with 100nM WM for 20min). Lipids were extracted and analyzed by HPLC. Panel shows one representative experiment out of two independent experiments.

P85^{-/-}-p55^{-/-}-p50^{-/-}-p85^{-/-} MEFS show defective signaling upon stimulation with PDGF-BB. The serine/threonine kinase Akt becomes activated in response to stimulation of PI3K (Brazil et al., 2002; Toker and Cantley, 1997). Phosphorylation of Akt on residue Ser473 reflects Akt activity and has been shown to correlate with the PIP₃ content of the cell. Serum-starved control and mutant cell pools were stimulated for 7min - 60min with various amounts of PDGF-BB with or without wortmannin pretreatment (100nM). The cells were lysed and the lysates were subjected to SDS-PAGE and western blot analysis using an anti-phospho-Akt antibody that specifically recognizes the protein when it is phosphorylated on residue serine 473. In order to normalize for total Akt in the gel, the blots were stripped and then reprobed with an anti-Akt antibody that recognizes Akt in its phosphorylated as well as unphosphorylated form. Consistent with the decreased PDGF-stimulated PIP₃ production in the mutant cells, there was also less PDGF-dependent phosphorylation of Akt both at subsaturating (1ng/ml) and saturating (10ng/ml) concentrations of PDGF-BB. Also the duration of Akt phosphorylation was reduced in mutant cells (Fig. 11a). PI3K has also been shown to be activated upon IGF-1 and EGF stimulation. Therefore, the phosphorylation of the PI3K target Akt was assessed after treatment of control and mutant cells with saturating concentrations of IGF-1 (20nM) and EGF (100ng/ml) for 5min. Akt phosphorylation in mutant cells was reduced compared to control cells using either IGF-1 or EGF as stimulants (Fig. 11b).

A. PDGF-dependent Akt Phosphorylation



B. IGF-1 and EGF-dependent Akt Phosphorylation



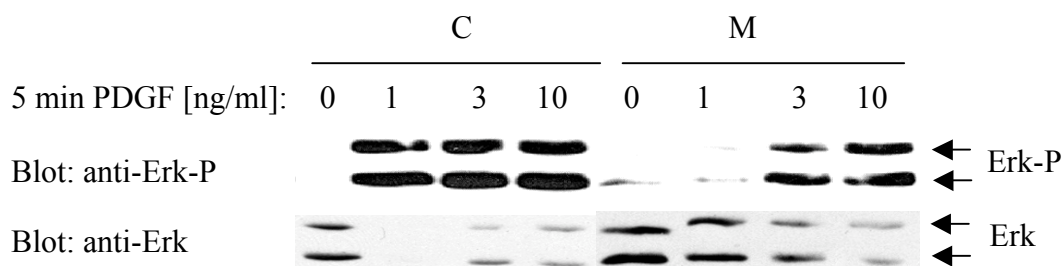
C: p85^{+/+}-p55^{+/+}-p50^{+/+}-p85^{-/-}

M: p85^{-/-}-p55^{-/-}-p50^{-/-}-p85^{-/-}

Fig. 11. p85 is required for optimal Akt phosphorylation upon treatment with PDGF, IGF-1 and EGF. MEFs with indicated genotypes were starved overnight and then stimulated with 1-10ng/ml PDGF for 7-60 min (A) or saturating amounts of PDGF (10ng/ml), IGF-1 (20nM) or EGF (100ng/ml) for 5min (B). Lysates were resolved by SDS-PAGE and immunoblotted with anti-Akt and anti-phospho-Akt antibodies. Blots are representative for at least 3 independent experiments.

There is evidence that Erk phosphorylation (which correlates with Erk activity) is inhibited by wortmannin when subsaturating concentrations of growth factors are used but is unaffected by wortmannin when saturating levels of growth factors are used (Duckworth and Cantley, 1997). Therefore, Erk phosphorylation was examined in control and mutant cells upon stimulation with various concentrations of PDGF-BB (ranging from 1-10ng/ml) for 5min. The serum-starved and PDGF-stimulated cells were lysed and the lysates were subjected to SDS-PAGE and western blot analysis using an anti-phospho-Erk antibody (that specifically recognizes the protein in its phosphorylated form) or with an anti-Erk antibody that recognizes Erk in its phosphorylated as well as unphosphorylated form. In agreement with wortmannin inhibition of Erk phosphorylation in cells stimulated with subsaturating concentrations of PDGF, we found that Erk phosphorylation was impaired in the mutant cells when a low level of PDGF (1ng/ml) was used. Saturating amounts of PDGF-BB (3-10ng/ml) led to normal Erk1/2 phosphorylation (Fig. 12).

Erk Phosphorylation upon PDGF



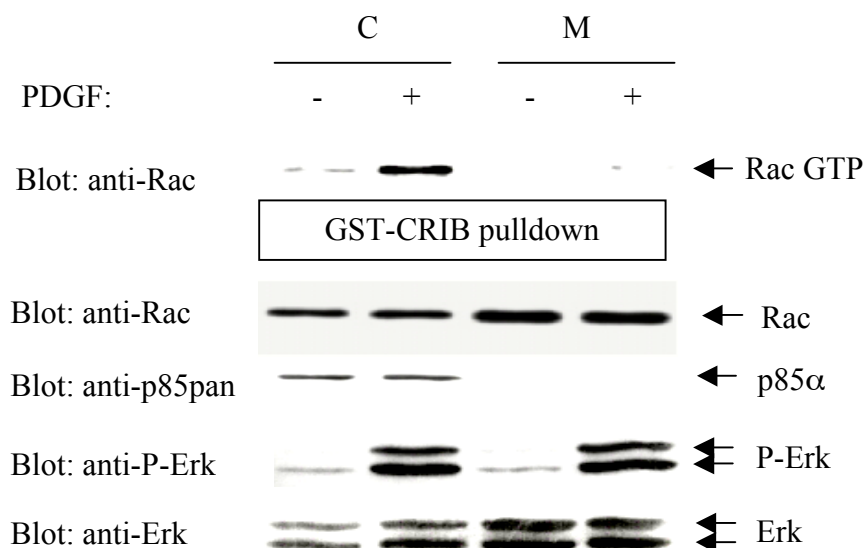
C: p85^{+/+}-p55^{+/+}-p50^{+/+}-p85^{-/-}

M: p85^{-/-}-p55^{-/-}-p50^{-/-}-p85^{-/-}

Fig. 12. p85 is required for Erk phosphorylation upon treatment with a low concentration of PDGF. MEFs with indicated genotypes were starved over night and then stimulated with 1, 3 or 10ng/ml PDGF for 5min. Lysates were resolved by SDS-PAGE and immunoblotted with anti-Erk and anti-phospho-Erk antibodies. *Note: The phosphorylation of Erk results in decreased blotting by the antibody that recognizes also the unphosphorylated form of Erk (lower panel).*

The small GTPase Rac has been reported to be downstream of PI3K. The activity of small G-proteins can be assessed by taking advantage of the fact that only the activated (GTP-bound) forms bind to their effectors. In the case of Rac, the Cdc42/Rac interactor binding (CRIB) domain of PAK65 fused to GST (GST-CRIB) can be used to specifically isolate the activated form of Rac. Control and mutant cells were transfected with HA-Rac. The serum-starved cells were stimulated with 50ng/ml PDGF-BB for 10min. The cells were lysed and the GTP bound form of Rac was affinity purified with GST-CRIB immobilized on beads. The pull down was then analyzed by western blot analysis probing with an anti-Rac antibody. The total amount of Rac (GDP-bound and GTP-bound forms) was examined by western blot analysis of the cell lysates. PDGF-dependent activation of Rac was impaired in the cells lacking all isoforms of p85 α and p85 β (Fig. 13). As an internal control, PDGF-dependent Erk phosphorylation was similar in the two cell types, as expected for saturating levels of PDGF (Fig. 14).

GTP -Loading of Rac upon PDGF



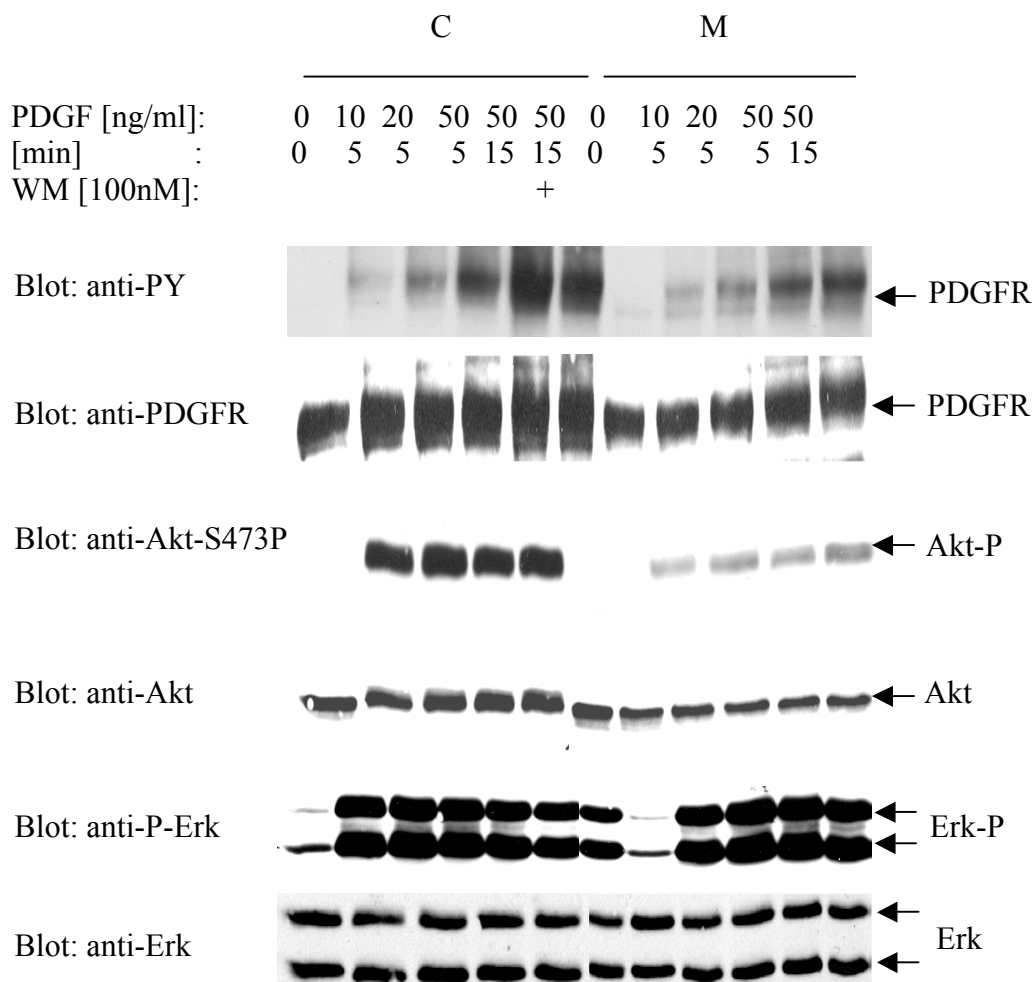
C: p85 α +/p55 α +/p50 α +/p85 β /-

M: p85 α /-p55 α /-p50 α /-p85 β /-

Fig. 13. p85 is required for PDGF-induced activation of Rac. Control (C) or mutant (M) cell pools with indicated genotypes were transfected with HA-Rac. The cells were starved and then stimulated for 10min with 50ng/ml PDGF. Equal amounts of lysates were subjected to in vitro binding assays with the immobilized CRIB domain of PAK65. Bound proteins were resolved by SDS-PAGE and immunoblotted with anti-Rac antibodies (Rac GTP). The levels of total Rac (Rac) and p85 are shown below. Equal stimulation was assessed by Erk activation.

After PDGF-BB treatment the PDGF receptor dimerizes and autophosphorylates on tyrosine residues. The tyrosine phosphorylation status of the receptor reflects its activity. The decreased Akt and Rac activation in the mutant cell pools might be due to loss of PI3K, but alternatively it could also be attributed to decreased input signal upstream of PI3K. Therefore the PDGF receptor levels and tyrosine phosphorylation were analyzed after PDGF-BB treatment. Serum-starved control and mutant cell pools were stimulated with various concentrations of PDGF-BB up to 15min. The cells were lysed and the lysates were examined by western blot analysis using anti-phosphotyrosine antibodies and anti-PDGF receptor antibodies to assess the phosphorylation status as well as protein levels of the receptor, respectively. PDGF receptor activation, was comparable between mutant and control cell pools after PDGF-BB stimulation up to 20ng/ml. At higher PDGF-BB doses, such as 50ng/ml, the control cells exhibited slightly higher PDGF receptor tyrosine phosphorylation. The discrepancy became more evident after 15min of PDGF-BB treatment. The same lysates were used to assess Akt and Erk phosphorylation by western blot analysis and showed Akt and Erk phosphorylation had already reached maximum stimulation at 10-20ng/ml PDGF-BB treatment (Fig. 14). The increased tyrosine phosphorylation of PDGF receptors in control cells could be because p85 protein binding to the receptor protects the phosphotyrosine residues from dephosphorylation. Alternatively, signals downstream of PI3K could inhibit phosphotyrosine phosphatases.

PDGF Receptor Phosphorylation and Protein Levels



C: p85^{+/+}-p55^{+/+}-p50^{+/+}-p85^{-/-}

M: p85^{-/-}-p55^{-/-}-p50^{-/-}-p85^{-/-}

Fig. 14. p85 is required for PDGF-induced activation of Akt. Control (C) or mutant (M) cell pools with indicated genotypes were starved and then stimulated with 10, 20 or 50ng/ml PDGF for indicated times +/- 100nM wortmannin. Lysates were resolved by SDS-PAGE and immunoblotted with anti-PDGFR Receptor, anti-Akt and anti-Erk antibodies. The activation of these proteins were assessed by anti-PY or phospho-specific antibodies.

MEFs lacking both p85 α and p55 α are not able to ruffle upon PDGF-BB treatment and are impaired in cell migration. PI3K has been reported to be necessary for PDGF-BB-induced lamellipodia formation (Severinsson et al., 1990b), (Cantley et al., 1991), (Wennstrom et al., 1994a), (Wennstrom et al., 1994c), (Kundra et al., 1994). Lamellipodia formation in mutant cells (p85 α ^{-/-}-p55 α ^{-/-}-p50 α ^{-/-}-p85 α ^{-/-}) was examined. Control and mutant cell pools were grown on coverslips, serum-starved overnight and then stimulated for 10min with 50ng/ml PDGF-BB with or without pretreatment with 100nM WM for 20min. The cells were then fixed and their actin cytoskeleton was stained with rhodamine phalloidin. PDGF-BB stimulated lamellipodia formation in control MEFs but not in the mutant MEFs (Fig. 15).

PDGF- induced Lamellipodia Formation

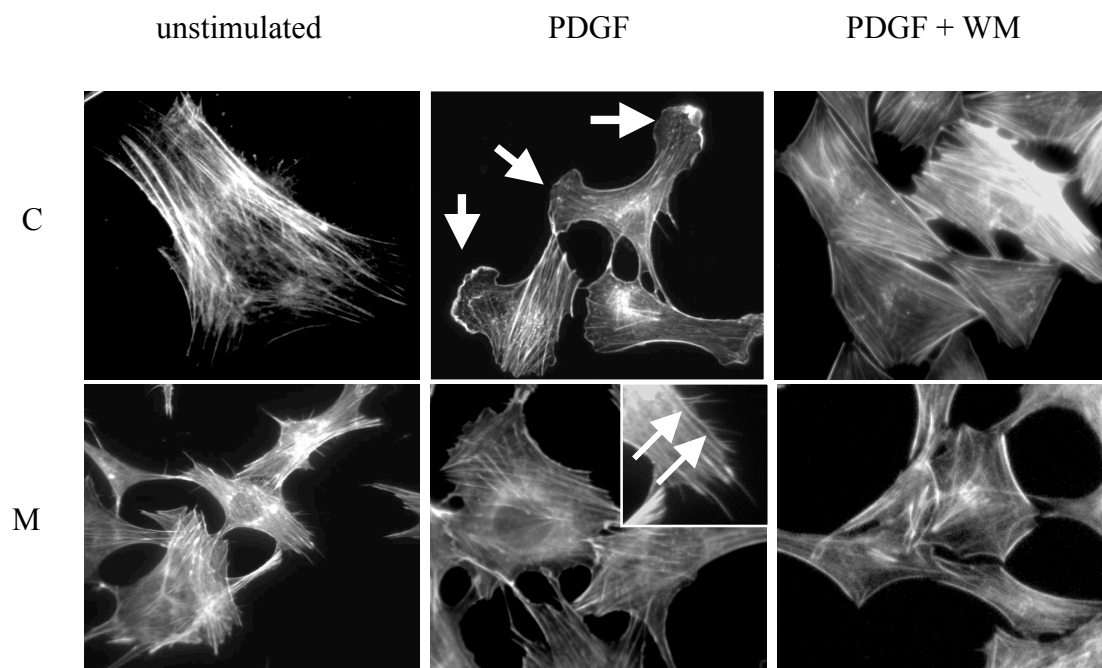


Fig. 15. p85 is required for PDGF-induced lamellipodia formation. Control (C) and mutant (M) cell pools were starved and then stimulated with 50ng/ml PDGF for 10min (+/- pretreatment with 100nM WM for 20min). The cells were fixed and actin structures were stained with rhodamine-phalloidin (arrows point to PDGF-induced lamellipodia formation in control cells but filopodia formation in mutant cells).

It has been shown that Rac is a crucial mediator of PDGF-BB-induced ruffling downstream of PI3K (Hawkins et al., 1995). We speculated that impaired PDGF-BB-induced Rac activation in p85^{-/-}-p55^{-/-}-p50^{-/-}-p85^{-/-} MEFs contributed to the defects in lamellipodia formation. We tested this hypothesis by overexpression of the Rac-specific GEF, Vav2. The mutant cell pool was cotransfected with Vav2 and Green Fluorescent Protein to allow visualization of the Vav2 transfected cells. The cells were starved and stimulated with 10ng/ml PDGF-BB. Cell ruffling was analyzed by live-cell microscopy or alternatively, the cells were fixed and the actin structures were stained with rhodamine phalloidin. Interestingly, overexpression of Vav2 circumvented the block in ruffling in the p85^{-/-}-p55^{-/-}-p50^{-/-}-p85^{-/-} cells and caused permanent lamellipodia formation even in the presence of 100nM wortmannin (Fig. 16). The lower panel of figure16 shows the “egg-fried” shape of cells known to be caused by Vav2 overexpression. The findings suggest that Vav2 acts downstream of PI3K or functions in a pathway that is parallel to PI3K.

Vav2 Overexpression-induced Lamellipodia Formation

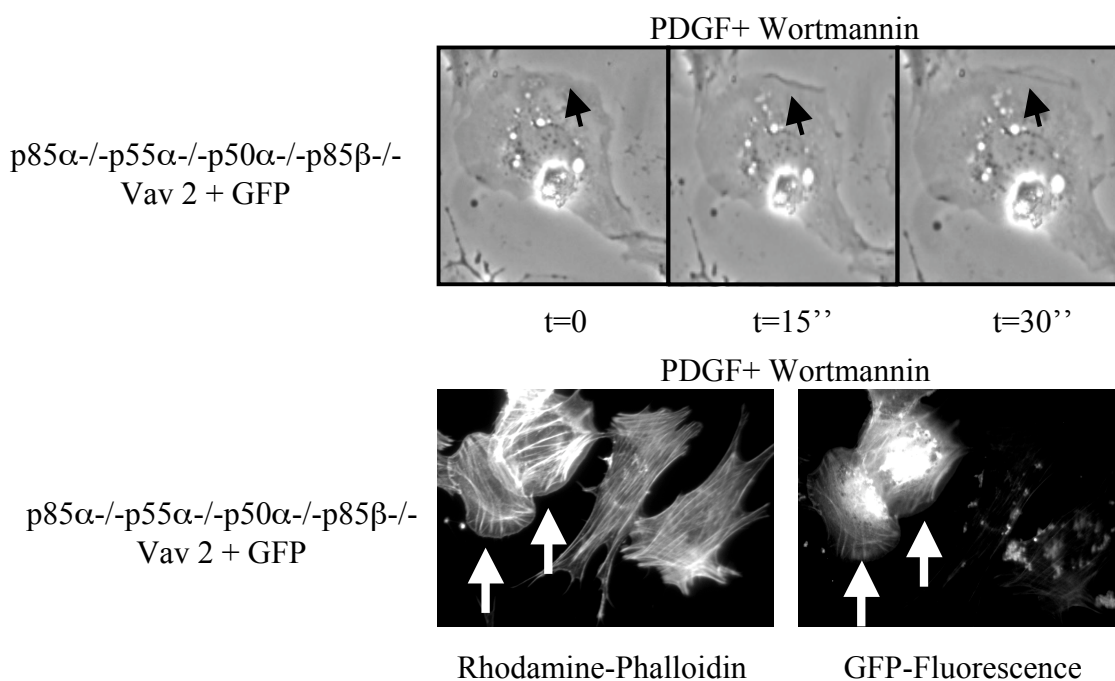
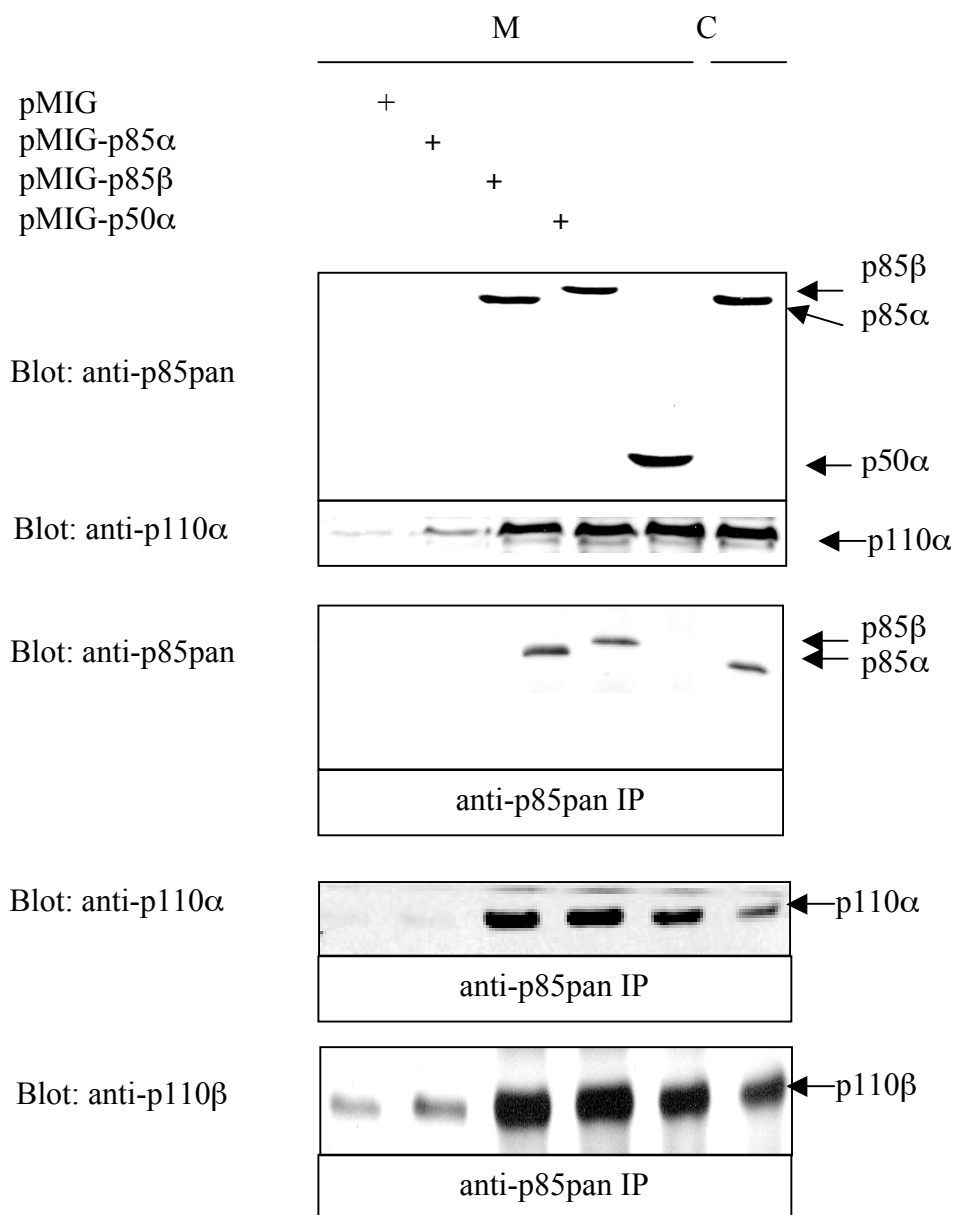


Fig. 16. WT-Vav-2 overexpression leads to lamellipodia formation in the absence of PI3K signaling. Upper panel: Mutant MEFs were cotransfected with WT-VAV-2 and GFP. The starved cells were stimulated with 10ng/ml PDGF + 100nM wortmannin, then cells were analyzed by time lapse microscopy. Pictures were taken every 15 seconds for 15min. A representative sequence is shown. Panels shows lamellipodia formation at leading edge. Lower panel: the cells were fixed and the actin structures were stained with rhodamine-phalloidin.

Previous studies using general PI3K inhibitors, dominant negative p85 or receptors lacking the p85 binding sites, did not address whether specific PI3K isoforms are required for cellular responses. In order to dissect p85 isoform specific functions in PDGF-BB induced lamellipodia formation a more physiological approach was taken in which fibroblasts with genetic ablation of various p85 isoforms were studied. Previously we analyzed lamellipodia formation upon PDGF-BB treatment of MEFs lacking either p85 α or p85 β . High variability among the individual cell pools in their capability to ruffle was seen. However, in contrast to p85 α -/-p55 α -/-p50 α -/-p85 β -/- MEFs it was clear that loss of p85 α isoforms alone or p85 β alone did not completely block PDGF-dependent lamellipodia formation (data not shown). Clonal variability can be circumvented by analyzing one cell pool into which the different p85 isoforms are added back. Furthermore, this approach allowed studying the effects of the small p85 γ isoform, p50 γ which lacks the domains that are present in the N-terminus of p85 α and p85 β . Therefore, in order to analyze the capability of the various p85 isoforms to mediate PDGF-BB induced ruffling, the expression of p85 α , p85 β or p50 γ was restored in the mutant (p85 α -/-p55 α -/-p50 α -/-p85 β -/-) MEFs. To do so, the mutant cell pool was infected with retroviral constructs for p85 α , p85 β or p50 γ . The infected cells were sorted by FACS analysis, since the retrovirus introduced an additional Green Fluorescent Protein (GFP) that could be used as a marker for infection. The infected cell pools were then analyzed for expression of p85 and p110 isoforms by western blot analysis. The levels of expression of the p85 α , p85 β and p50 γ proteins following retroviral infection and sorting (FACS) of infected cells were in a range similar to the expression of p85 α in the control cells based on blotting with the anti-pan p85 antibody (Fig. 17, upper panel). (However, this antibody detects p85 α somewhat better than p85 β implying that p85 α expression is higher than the other isoforms.) The protein levels of p110 α and p110 β were either examined on lysates (only p110 α) or on co-immunoprecipitates with the anti-p85pan antibody using anti-p110 α or anti-p110 β antibodies. The protein levels of p110 α and p110 β (that were decreased in the p85 α -/-p55 α -/-p50 α -/-p85 β -/- cell pool in comparison to the control pool) increased to control levels upon re-introduction of the various p85 isoforms (Fig.17, middle and lower panels).

Retroviral Restoration of p85 and p110 Protein Levels



M: p85 Δ Δ -p55 Δ Δ -p50 Δ Δ -p85 Δ Δ -
 C: p85 Δ Δ +p55 Δ Δ +p50 Δ Δ +p85 Δ Δ -

Fig. 17. Retroviral restoration of p85. Mutant (M) cell pools were infected with retroviral pMIG-constructs to restore expression of p85 Δ , p85 Δ or p50 Δ similarly to the control (C) cell pool. The infected cells were lysed and the protein levels were examined by western blot analysis of the lysates or, alternatively, p85/p110 complexes were immunoprecipitated using the anti-p85pan antibody and then examined by western blot analysis.

Next, the PDGF-BB- and IGF-1-induced lamellipodia formation was examined in the various add-back cells. The cells were grown on coverslips, starved overnight and then stimulated with 50ng/ml PDGF-BB or 20nM IGF-1. Lamellipodia formation was assessed by time lapse microscopy of live cells. Consistent with the unimpaired lamellipodia formation of p85^{-/-} or p85^{-/-} MEFs, retroviral reintroduction of p85⁺ or p85⁺ into p85^{-/-}-p55^{-/-}-p50^{-/-}-p85^{-/-} MEFs to endogenous levels rescued the ruffling defect. Surprisingly, the expression of the smaller p85 isoform, p50⁺, was also sufficient to rescue the defect (Fig. 18).

Mutant cell pool infected:	PDGF-BB	IGF-1
pMIG	1.9%	1.3%
pMIG-p85 ⁺	3.9%	7.1%
pMIG-p85 ⁺	9.5%	13.1%
pMIG-p50 ⁺	13.1%	6.1%

Fig. 18. Various p85 isoforms mediate PDGF-/IGF-1-induced circular ruffling. Mutant (p85^{-/-}-p55^{-/-}-p50^{-/-}-p85^{-/-}) cell pools were infected with retroviral pMIG-constructs to restore expression of p85⁺, p85⁺ or p50⁺ similarly to the control (p85^{+/+}-p55^{+/+}-p50^{+/+}-p85^{-/-}) cell pool. Mutant and control cells were plated on coverslips, starved over night and then stimulated with either 50ng/ml PDGF-BB or 20nM IGF. Pictures were taken every 15sec for 2h. The number of cells exhibiting circular ruffles were counted.

The migration of mutant fibroblasts was examined by time-lapse microscopy of live cells. Control and mutant cells were plated on coverslips (less than 12h) and stimulated with 50ng/ml PDGF-BB (uniform stimulus) in DMEM containing 0.5% BSA. Pictures were taken every 5min for 12h and the frames were combined to form a movie. Following PDGF-BB stimulation, the control cells migrated randomly across the coverslip and exhibited broad lamellae at the leading edge and a thin tail at the trailing end that eventually retracted. In contrast, the mutant cells were unable to polarize their front, instead they formed many filopodia that caused frequent changes of direction during migration. In addition, the mutant cells were unable to detach their trailing end and thus remained stationary. Figure 19 shows a frame of a moving control and mutant cell, each.

PDGF-induced Cell Polarization

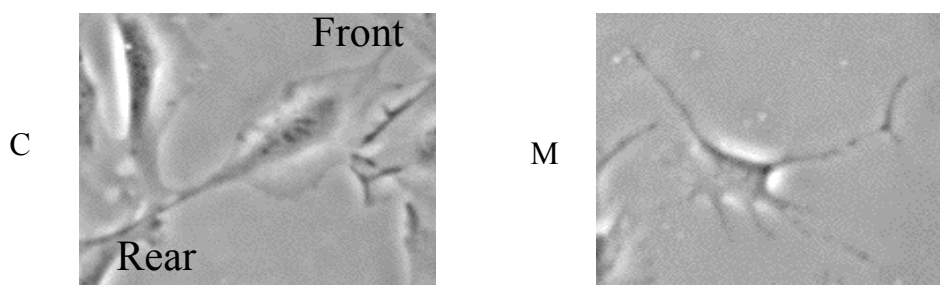
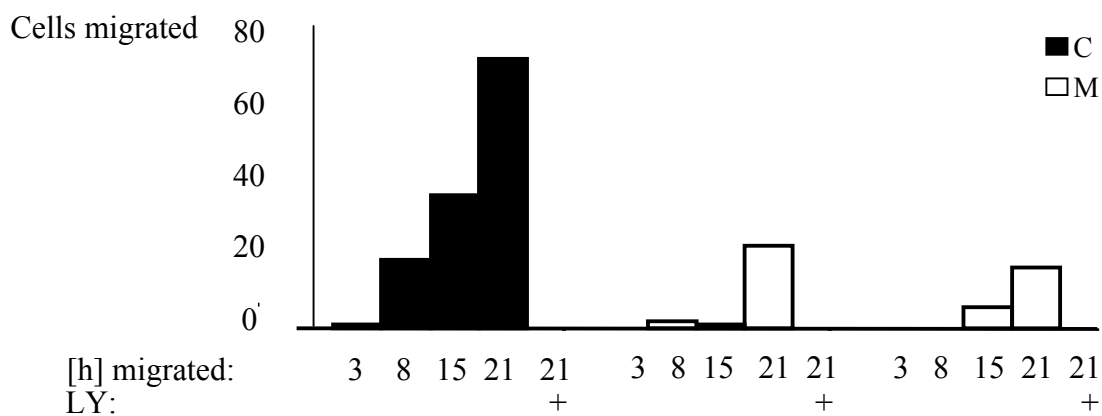
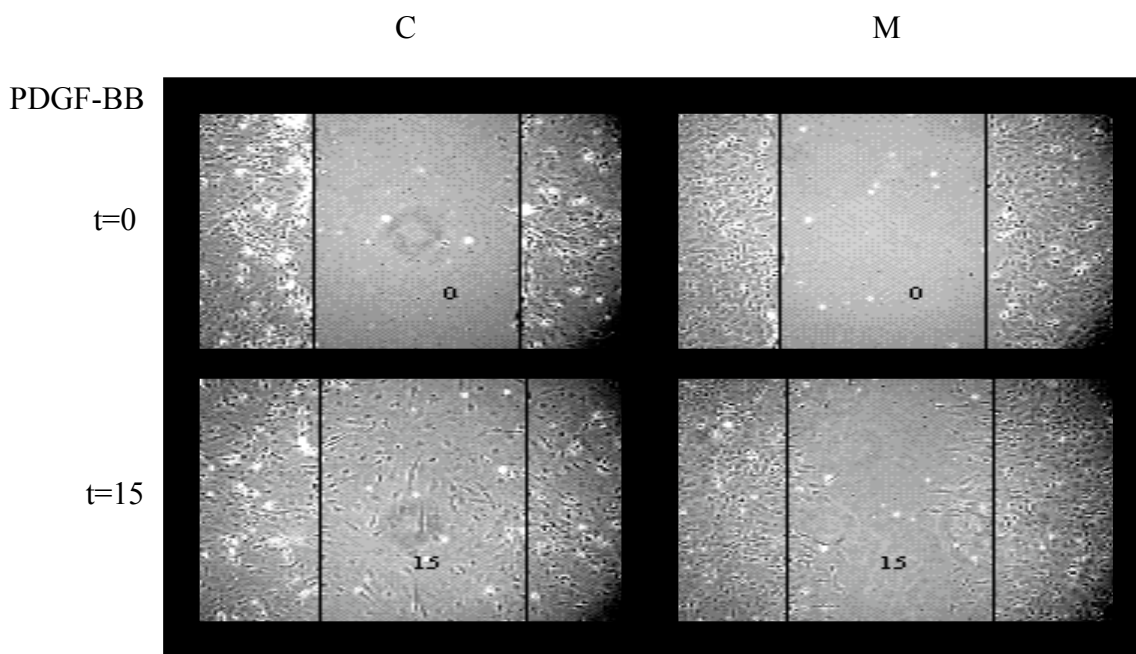


Fig. 19. p85 is required for PDGF-induced Polarization. Control (C) and mutant (M) cell pools were stimulated with 50ng/ml PDGF in DMEM containing 0.5% BSA. Pictures of moving cells were taken every 5min for 12h. Frames show moving cells after about 4h.

Cell migration was also assessed in wound healing assays. Control and mutant cell pools were grown to confluency and then serum-starved overnight. The next day, a wound was scratched into the confluent monolayer and a homogenous stimulus was applied, such as PDGF-BB with or without the presence of the stable PI3K inhibitor LY294002. Pictures were taken frequently to observe how fast the cells migrated into the wound. In the presence of PDGF-BB, two independent mutant cell pools filled the wound to a much slower rate than the control cells. Both, the PDGF-BB-induced migration of the mutant and control cell pools were completely inhibited by the PI3K inhibitor LY294002 (Fig. 20).

PDGF-BB-induced Cell Migration



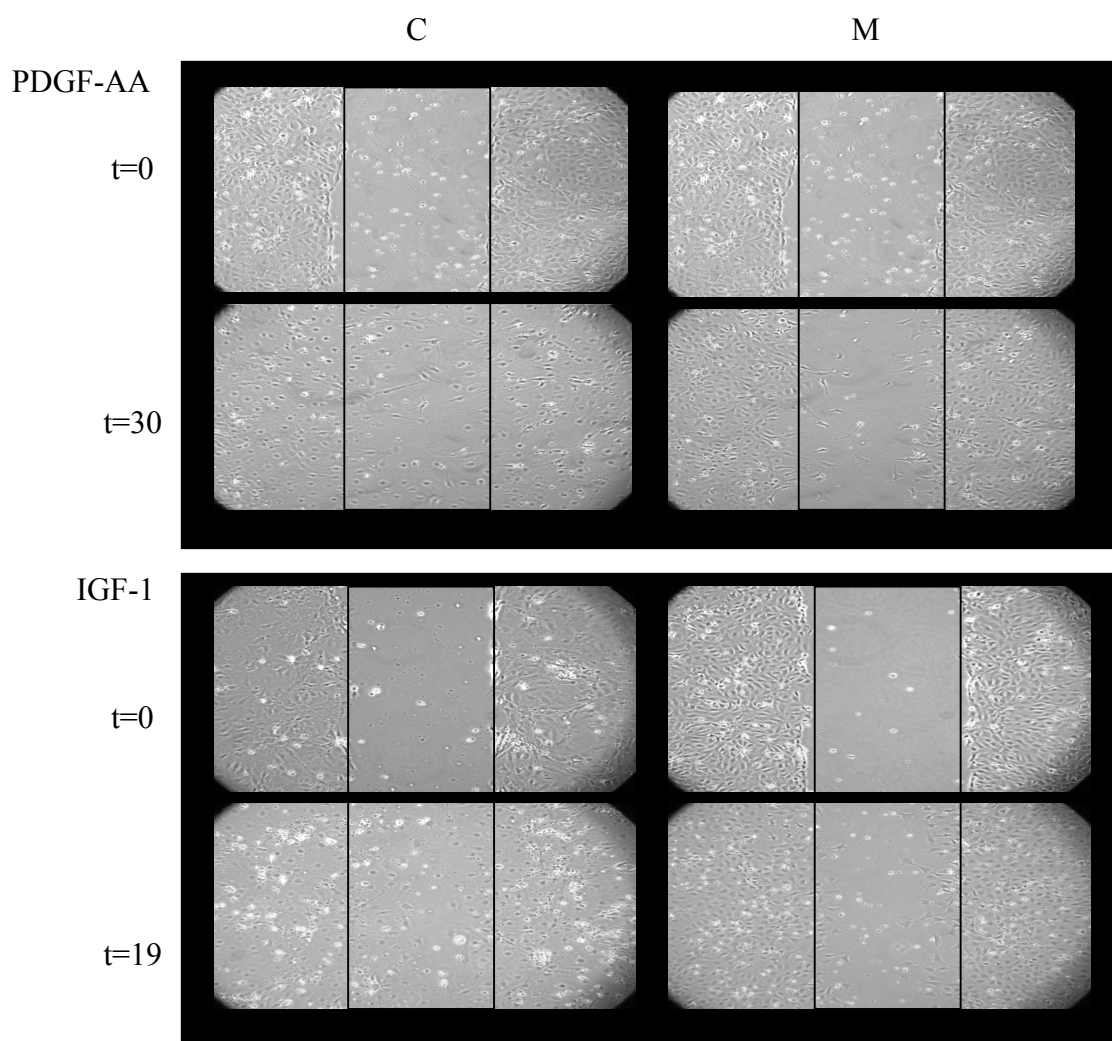
C : p85^{+/+}-p55^{+/+}-p50^{+/+}-p85^{-/-}

M: p85^{-/-}-p55^{-/-}-p50^{-/-}-p85^{-/-}

Fig. 20. p85 is required for PDGF-BB-induced Cell Migration. Mutant (M) and control (C) cell pools were grown to confluency and then starved. A wound was applied with a pipette tip and the floating cells were washed away. DMEM with 10ng/ml PDGF-BB +/- 10 μ m LY was added and the wounds were photographed at indicated times. The upper panel shows a representative photograph at t=0h (upper) and t=15h (lower). The lower panel shows the quantification of one representative experiment.

Next, using the same procedure, the cell motility in the presence of PDGF-AA, IGF-1 and EGF was analyzed. PDGF and IGF-1 accelerated migration of the control cells into the wound but failed to stimulate migration of the p85^{-/-}-p55^{-/-}-p50^{-/-}-p85^{-/-} cell lines into the wound (Fig 21 and 23).

PDGF-AA- and IGF-1-induced Cell Migration

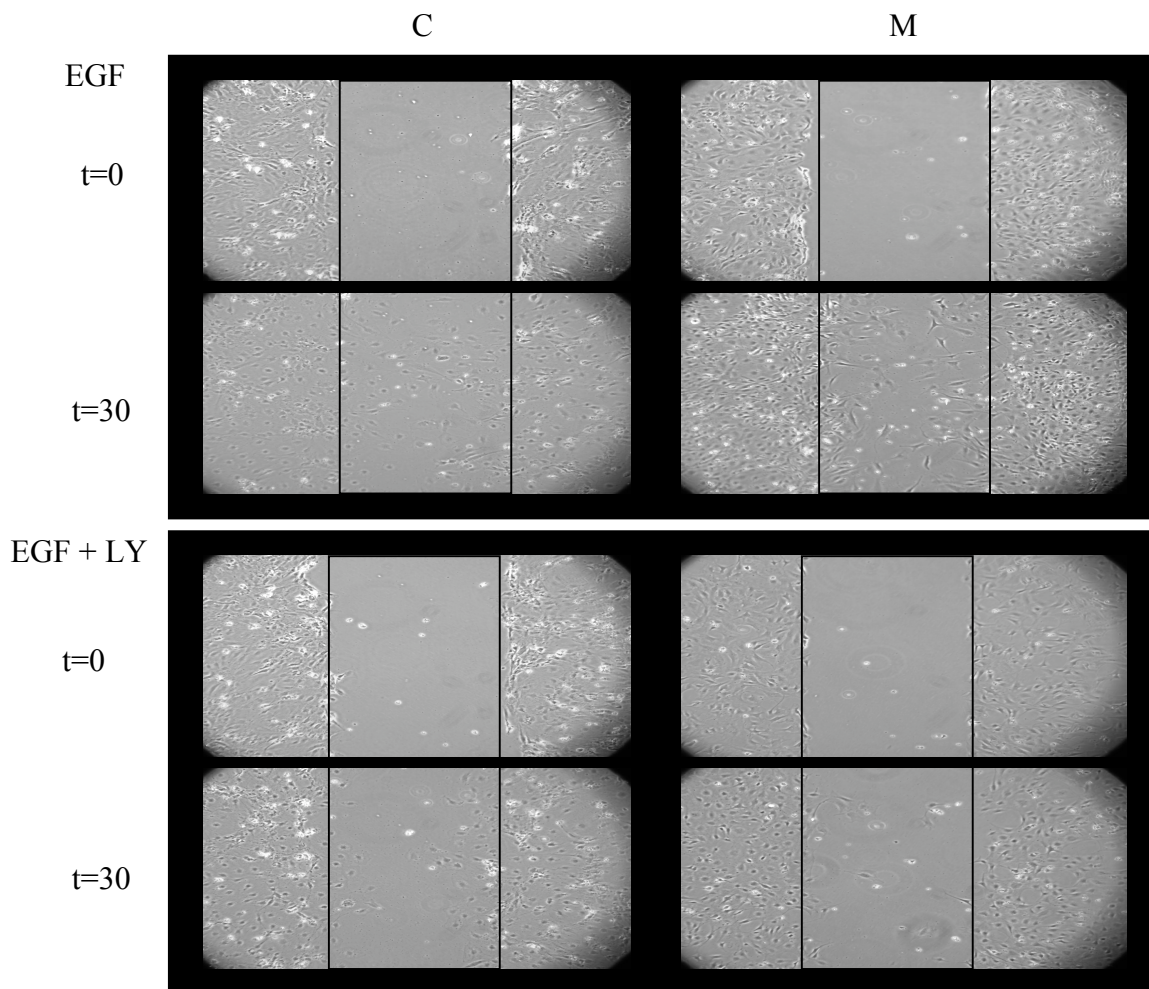


M: p85^{-/-}-p55^{-/-}-p50^{-/-}-p85^{-/-}
 C: p85^{+/-}-p55^{+/-}-p50^{+/-}-p85^{-/-}

Fig. 21. p85 is required for PDGF-AA- and IGF-1-induced Cell Migration. Mutant (M) and control (C) cell pools were grown to confluency and then starved. A wound was applied with a pipette tip and floating cells were washed away. DMEM with 100ng/ml PDGF-AA (upper panel) or 50nM IGF-1 (lower panel) was added and the wounds were photographed at indicated time points. The panels show a representative experiment out of three experiments, each.

In contrast, there was little difference between control cells and mutant cells when the migration was carried out in the presence of EGF (Fig. 22, 23).

EGF-induced Cell Migration



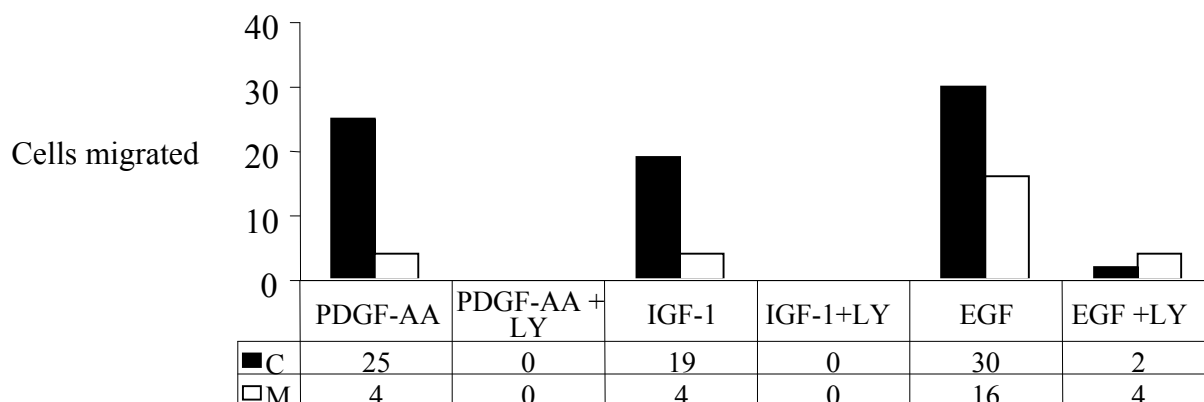
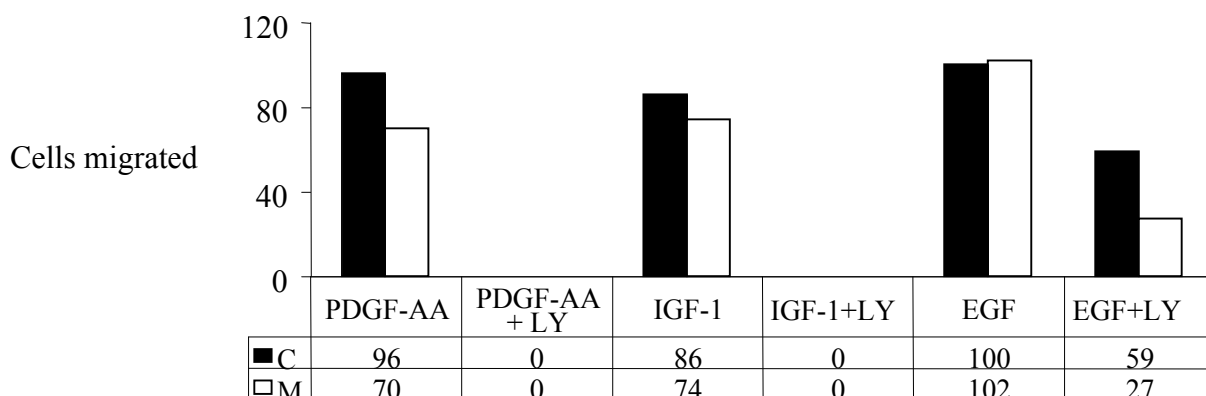
C: p85^{+/+}-p55^{+/+}-p50^{+/+}-p85^{-/-}

M: p85^{-/-}-p55^{-/-}-p50^{-/-}-p85^{-/-}

Fig. 22. PI3K activity but not p85 are required for EGF-induced cell migration. Mutant (M) and control (C) cell pools were grown to confluency and then starved. A wound was applied with a pipette tip and floating cells were washed away. DMEM with 100ng/ml EGF +/- 10 μ M LY was added and wounds were photographed at indicated time points. The panels show a representative experiment out of three experiments, each.

Cell migration induced by PDGF and IGF-1 was inhibited completely with LY294002, but only partially in the EGF stimulated conditions. These data suggest that class Ia PI3K is a necessary component to transmit cell motility signals from PDGF-BB/-AA and IGF-1 whereas EGF utilizes PI3K dependent and independent signaling pathways to induce cell migration.

Class Ia PI3K-dependent Cell Migration



C: p85^{+/+}-p55^{+/+}-p50^{+/+}-p85^{-/-}

M: p85^{-/-}-p55^{-/-}-p50^{-/-}-p85^{-/-}

Fig. 23. p85 is required for Cell Migration. Mutant (M, white bars) and control (C, black bars) cell pools were grown to confluency and then starved over night. A wound was applied with a pipette tip and the floating cells were washed away. DMEM (+/- 10 μ M LY) with 100ng/ml PDGF-AA, 50nM IGF-1, 100ng/ml EGF was added and cells migrated into the wounds were counted after 19h (IGF-1) and 30h (PDGF-AA, EGF). The graphs show the quantification of a representative experiment for each condition out of 3 independent experiments. The upper panel shows the number of cells that migrated into the wound, whereas the lower panel shows the number of cells that migrated into the middle third of the wound.

DISCUSSION

Mice with combined loss of p85 α and p85 β gene products (p85 α ^{-/-}p55 α ^{-/-}p50 α ^{-/-}p85 β ^{-/-}) exhibit severe developmental defects that result in embryonic lethality (described in the previous chapter). In order to elucidate signaling defects due to the loss of PI3K at the cellular level, mouse embryonic fibroblasts (MEFs) from mutant (p85 α ^{-/-}p55 α ^{-/-}p50 α ^{-/-}p85 β ^{-/-}) and control (p85 α ^{+/+}p55 α ^{+/+}p50 α ^{+/+}p85 β ^{-/-}) embryos at E8-9 were isolated. The cells proliferated in culture for no more than 5 passages before they adopted a typical senescent morphology. This finding is in agreement with reports that PI3K inhibitors can induce a senescence-like phenotype in wild-type MEFs that is associated with upregulation of p27 (Kip1) (Collado et al., 2000). By retroviral introduction of the SV40 large T antigen we could rescue the p85 α ^{-/-}p55 α ^{-/-}p50 α ^{-/-}p85 β ^{-/-} MEFs and establish immortalized, stable cell lines: three mutant p85 α ^{-/-}p55 α ^{-/-}p50 α ^{-/-}p85 β ^{-/-} cell pools and one control p85 α ^{+/+}p55 α ^{+/+}p50 α ^{+/+}p85 β ^{-/-} cell pool were generated this way. Western blot analysis revealed the complete loss of p85 α and p85 β in these mutant cells (Fig. 8a). The smaller p85 α splice variants are not ubiquitously expressed (Inukai et al., 1997) and therefore not detectable in mutant and control cells. Surprisingly, western blot analysis with an anti-p55 α antibody showed expression of p55 α in the mutant cell pools. As expected, p55 α expression was not found in the control cell pool (Fig. 8a). It is not clear when and how p55 α was upregulated in the p85 α ^{-/-}p55 α ^{-/-}p50 α ^{-/-}p85 β ^{-/-} cells but it most likely fulfills a compensatory function. Probably, only those cells that express p55 α were selected during the culturing and immortalization process, since it provides some PI3K activity that could lead to a growth advantage in comparison to cells that do not upregulate p55 α . Interestingly, there is recent evidence that p55 α can interact with the retinoblastoma tumor suppressor protein (Rb) via its unique N-terminal sequence. Rb is a cellular target of the SV40 large T antigen (Xia et al., 2003) and a crucial regulator of the G1/S transition in mammalian cells (for review: (Harbour and Dean, 2000)).

Mutant cell pools exhibited greatly reduced, but detectable PI3K activity associated with the anti-p85pan antibody precipitate (Fig. 8b) The residual PI3K activity can be

attributed to p55/p110 complexes, since this antibody cross reacts with p55 to some extent. The stability of p110 is strongly dependent on its association with p85 (Yu et al., 1998). Loss of p85 or combined loss of p85 with its smaller isoforms p55/p50 resulted in greatly reduced levels of p110 protein in muscle and liver (Terauchi et al., 1999), (Fruman et al., 2000). P110 protein levels were assessed in p85^{-/-}-p55^{-/-}-p50^{-/-}-p85^{-/-} MEFs by western blot analysis of anti-p110 immunoprecipitates. In comparison to control cell pools, p110 levels were greatly reduced but still remained detectable in the mutant cell pools (Fig. 9a). We assume that the p55 detected in the mutant cell pools contributes to the stabilization of the remaining p110. Similarly, the PI3K activity associated with the anti-p110 immunoprecipitate was found greatly reduced, but still detectable in the mutant cell pools (Fig. 9b).

The generation of PI3K lipid products can be assessed in *in vitro* kinase assays on anti-phosphotyrosine immunoprecipitates after PDGF stimulation. Alternatively, PIP₃ production can be directly measured by ³²P-ortho-phosphate labeling, *in vivo*. Both experiments showed substantially reduced, albeit still detectable PI3K activity in the mutant cell pools in comparison to control cell pools (Fig. 10a and 10b, respectively). This activity could be completely inhibited by treating cells with wortmannin. Class II PI3K is also activated upon PDGF-BB treatment (Arcaro et al., 2000), *in vitro* studies showed that the class II PI3K C2 can utilize PI, PI4P and to a much lesser extent PI-4,5-P₂ as substrates (Domin et al., 1997). However, class II PI3K C2 is less sensitive to wortmannin than p110: whereas treatment with 100nM wortmannin (concentration used in our experiments) completely blocks p110 kinase activity, the IC₅₀ of class II PI3K (C2) has been determined to be 420nM, with maximal inhibition only being obtained using WM at 10mM. (Domin et al., 1997). Since PDGF-BB-induced PI-3,4-P₂ and PIP₃ production was completely blocked upon pretreating cells with 100nM wortmannin, it is unlikely that PI3K C2 plays a major role in generating these phosphoinositides upon PDGF-BB stimulation in our cell pools under these experimental conditions. Though equally sensitive to wortmannin as class Ia PI3K, class II PI3K C2 can utilize PI and PI4P but not PI-4,5-P₂ (Arcaro et al., 1998). In the mutant cell pools the PDGF-BB-induced PIP₃ production is therefore most likely attributed to p55/p110, whereas the

PDGF-BB-induced PI-3,4-P₂ generation might be attributed to p55/p110 as well as class II PI3K C2.

Akt, a major downstream target of PI3K is recruited to the plasma membrane via the interaction of its PH domain with PI-3,4-P₂ and/or PIP₃. At the plasma membrane Akt is phosphorylated on threonine 308 and serine 473 in a PI3K-dependent manner, and becomes fully activated (Alessi et al., 1997). Since PDGF-BB-induced PI-3,4-P₂ and PIP₃ production were greatly reduced in the mutant cell pool *in vivo*, it was not surprising that this was reflected in the PDGF-BB-induced phosphorylation of Akt. Short term and long term stimulation with sub-saturating as well as saturating doses of PDGF-BB both resulted in diminished Akt phosphorylation in the mutant cells (Fig 11). It was surprising, however, that despite the substantial loss of PI3K isoforms, the reduction in Akt phosphorylation was relatively mild. This can be explained by the model that the amplification of signal at the level of PI3K due to the relative large amount of PIP₃ produced by each PI3K molecule could result in a milder defect downstream (e.g. at the level of Akt phosphorylation) of the signaling cascade (Park et al., 2003).

PDGF receptor activation was assessed by analyzing the phosphotyrosine status of the receptor. Treatment of mutant and control cell pools with up to 20ng/ml PDGF-BB resulted in similar amounts of PDGF receptor tyrosine phosphorylation among the cell pools. However, at higher PDGF-BB concentrations, such as 50ng/ml, the control cells exhibited a slightly higher tyrosine phosphorylation of the receptor. This became even more evident at a later time point (15min). The differences might be due to the ability of p85 to bind to phosphotyrosine residues on the PDGF receptor and protect them from phosphotyrosine phosphatases. However, the decreased PDGF receptor phosphorylation observed in the mutant cells with prolonged treatment with saturating PDGF can not account for Akt and Erk phosphorylation defects, since those defects are seen at subsaturating concentrations of PDGF-BB, such as 1ng/ml and at short incubation times. In contrast to Akt, Erk phosphorylation is not PI3K-dependent at high doses of PDGF-BB. But at lower doses of PDGF-BB (such as 1ng/ml) Erk phosphorylation is also diminished in mutant cells compared to control cells (Fig. 12). This finding is in agreement with previous results that the PI3K-dependency of Erk activation correlates with the strength of stimulus (Duckworth and Cantley, 1997). At higher PDGF-BB

concentrations, mutant and control cell pools exhibit similar Erk phosphorylation. At low concentrations of PDGF-BB (such as 1ng/ml), PI3K-dependent and independent pathways are necessary for Erk phosphorylation, whereas at higher PDGF-BB concentrations the PI3K-independent pathway is sufficient to cause maximal Erk phosphorylation. In support of this notion, wortmannin treatment does not block PDGF-induced Erk phosphorylation at high doses of PDGF-BB.

The small GTPase Rac is activated by PH domain-containing GEFs. PIP₃ activates a subgroup of Rac-specific GEFs. PDGF-BB-stimulated GTP loading of Rac is greatly diminished in p85^{-/-}-p55^{-/-}-p50^{-/-}-p85^{-/-} cells (Fig. 13). Since Rac is a crucial mediator of PDGF-induced lamellipodia formation, it was not surprising that the mutant cell pools showed impaired ruffling upon PDGF stimulation (Fig. 15). Similar to MEFs that express a mutant PDGF receptor that cannot bind to and thus activate PI3K (Heuchel et al., 1999), p85^{-/-}-p55^{-/-}-p50^{-/-}-p85^{-/-} MEFs showed a total absence of circular actin ruffles upon PDGF-BB treatment. These findings suggest that PI3K is a necessary mediator of PDGF-BB induced lamellipodia formation. P85^{-/-}-p55^{-/-}-p50^{-/-}-p85^{-/-} fibroblasts also fail to ruffle upon PDGF-AA or IGF-1 stimulation. This finding is in agreement with reports that IGF-1-induced ruffling is completely blocked by wortmannin treatment or overexpression of dominant negative p85 (Kotani et al., 1994). In order to test the hypothesis that impaired Rac activation is the cause of the inability of the p85^{-/-}-p55^{-/-}-p50^{-/-}-p85^{-/-} cell pools to ruffle, Rac activation was driven by overexpressing the Rac-specific GEF Vav2. Vav2 overexpression in the mutant cells rescued the ruffling defect even in the presence of wortmannin (Fig. 16). Vav2 overexpression in NIH 3T3 fibroblasts has been shown to result in Rac activation as judged by increased Rac-GTP levels and lamellipodia formation (Marignani and Carpenter, 2001). Marignani et al further showed that Src activity is necessary for Vav2 activity. We detected no differences in src phosphorylation between PDGF-stimulated mutant and control cell pools (data not shown). In agreement with this, wortmannin did not affect Vav-2 dependent Rac activation or lamellipodia formation. These data show that src activity but not PI3K is necessary for Vav-2 induced lamellipodia formation. Although the mutant cells were unable to undergo Rac-activated lamellipodia formation, PDGF treatment caused the formation of extensive filopodia in the mutant cell pools (Fig. 15). This

finding contradicts reports from Jimenez et al that suggest that PDGF-induced filopodia formation is not dependent on PI3K activity but depends on p85 β protein (Jimenez et al., 2000). Controlled filopodia formation is a Cdc42 dependent process and plays a crucial role in maintaining cell polarity and localization of the lamellipodial activity to the leading edge of a cell (Nobes and Hall, 1999).

Time lapse video microscopy reveals that PDGF-stimulated mutant cells form extensive filopodia but are unable to polarize and form a single leading edge (Fig.19). Instead of moving decisively in one direction, they frequently change directions. In addition to the polarization defect, the mutant cell pools are unable to retract their trailing edge. As a consequence, the migration of the mutant cells is severely reduced as also analyzed in woundhealing assays. This migration defect was not only observed upon PDGF-BB stimulation (Fig. 20), but also upon PDGF-AA stimulation (which only activates PDGF receptor β homodimers) (Fig. 21). These findings are coherent with cell migration defects seen in cells expressing mutant PDGF receptors β or β which do not bind PI3K (Kundra et al., 1994), (Wennstrom et al., 1994c), (Heuchel et al., 1999), (Rosenkranz et al., 1999). Furthermore, mutant cells exhibited migration defects upon IGF-1 (Fig. 21 lower) and to a lesser extent, upon EGF stimulation (Fig. 22). While PI3K is a major mediator of PDGF- and IGF-1-induced migration it appears to only play a minor role in EGF-induced migration. This is supported by our finding, that LY294002 treatment causes only a partial inhibition in EGF-induced migration in the control cell pool in comparison to the 100% block in PDGF- and IGF-1-induced migration in the same cells (Fig. 23).

The migration defect in the mutant cells may in part be due to reduction in Akt activation in these cells. There is recent evidence that Akt (independently of Rac) can phosphorylate and thereby activate p21 Pak (Zhou et al., 2003), (Tang et al., 2000). Pak has been shown to be involved in processes such as the formation of adhesions at the leading edge, the detachment of the trailing end and cell contraction (Kiosses et al., 1999). While the phosphorylation of Pak by Akt might not be Rac dependent, the phosphorylation of Akt itself might be dependent on Rac activity. Consistent with the hypothesis of Rac being upstream of Akt, hematopoietic stem/progenitor cells lacking

Rac2 exhibited decreased Akt phosphorylation upon treatment with stem cell factor (Gu et al., 2003).

Retroviral add-back of p85 α , p85 β or p50 α into a mutant cell pool (p85 α ^{-/-}p55 α ^{-/-}p50 α ^{-/-}p85 β ^{-/-}) restored p85 expression to a level similar to that observed in the control cell pool (p85 α ^{+/+}p55 α ^{+/+}p50 α ^{+/+}p85 β ^{-/-}). The add-back of these proteins also raised the levels of p110 α and p110 β proteins back to normal (Fig. 17). As anti-p85pan antibody recognizes p85 α to a lesser degree than p85 α /p50 α , we estimate that the p85 α protein levels in these add-back cells were somewhat higher than p85 β protein levels. Consistent with this, all p85 isoforms restored Akt phosphorylation upon PDGF treatment with p85 α showing the weakest effect. The Akt phosphorylation correlated with the expression level of the p85 isoforms (data not shown). Furthermore, PDGF induced Akt activation was not dependent on the N-terminal domains of p85 α or p85 β . In contrast to p85 α ^{-/-}p55 α ^{-/-}p50 α ^{-/-}p85 β ^{-/-} cells, the mutant cell pools with either p85 α , p85 β or p50 α were able to undergo PDGF- or IGF-1-induced lamellipodia formation (Fig. 18). The results show clearly that the small p85 α isoform p50 α is able to mediate PDGF- or IGF-1-induced lamellipodia formation. Therefore, the interaction between Rac-GTP or Cdc42-GTP with the Rho-GAP domain of p85 α / β is not essential for PDGF- or IGF-1-induced lamellipodia formation in these cells under our experimental conditions.

Attempts to rescue the PDGF-dependent migration with the retroviral add-back approach have been failed. This can be attributed to many reasons: (1) the migration defects are not due to loss of p85 isoforms which is unlikely given the supportive *in vitro* data (2) the mutant cell pools have undergone further changes and restoration of p85 expression is no longer sufficient to restore migration in these cells. In order to address this problem, we will analyze PDGF-induced migration by using mouse embryonic fibroblasts with two floxed alleles of p85 α on a p85 α null background in which the p85 α gene can be acutely deleted by the expression of Cre-recombinase. Retroviral expression of the individual p85 isoforms before induction of Cre-recombinase will lead to an acute switch from the endogenous p85 α /p55 α /p50 α isoforms (which are encoded by the p85 α gene) to either p85 α , p55 α , p50 α or p85 β which is expressed from a retroviral vector. By doing so, compensatory events should be minimized. Furthermore, p110 levels should

remain stable in these cell pools as at no stage is there large change in the total level of p85 proteins.

In summary, we have shown that class Ia PI3K is necessary for PDGF- and IGF-1-induced / Rac-mediated lamellipodia formation. The interaction between Rac-GTP or Cdc42-GTP with the Rho-GAP domain of p85 α/β is not essential for this cellular response. Furthermore, class Ia PI3K is necessary for PDGF- and IGF-1-induced cell polarization and migration. In contrast, class Ia PI3K plays only a minor role in EGF-induced cell motility.